ADDITIVELY MANUFACTURED LATTICE STRUCTURES FOR PRECISION ENGINEERING APPLICATIONS

Waiel A. Elmadih[1], Wahyudin P. Syam[1], Ian Maskery[2] and Richard Leach[1]
[1]Manufacturing Metrology Team
[2]Centre for Additive Manufacturing
University of Nottingham
Nottingham, NG7 2RD, UK

INTRODUCTION

Additive manufacturing (AM) is limited by fewer design constraints than conventional manufacturing [1]. Therefore, AM provides higher design flexibility and allows fabrication of highly complex geometries, for example, lattice structures. Compared to solid structures, lattice structures allow designs that incorporate highly-tailored mechanical properties so that the requirements of applications are met with efficient use of resources [2].

Representative stress-strain curves for solid and lattice structures are shown in **Error! Reference source not found.**. In **Error! Reference source not found.**, the area under the curve up to the densification strain is the energy absorbed per unit volume of material. The energy absorption is small for a solid, compared to lattice structures that benefit from long plastic plateau regions in their stress-strain curves.

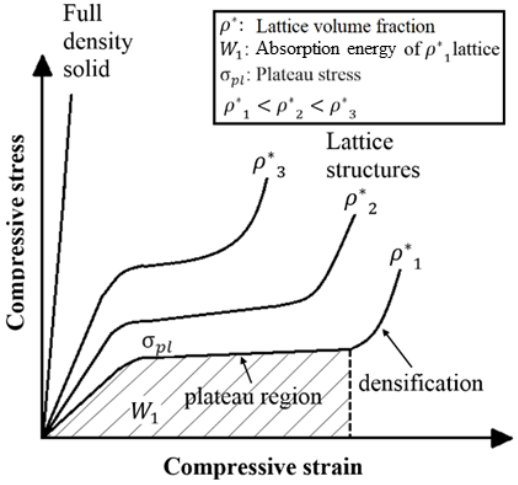

FIGURE 1. Representative stress-strain curves of a full density solid and lattice structures of different density fraction, adapted from [1].

The length of this plateau region, and the stress at which it occurs, depends on the lattice material, volume fraction, unit cell configuration, and the number of lattice cells in a structure [1]. As such, with the same total volume, different lattice configurations can have different mechanical properties. There has been considerable research focus on the manufacturability and strength-to-weight ratio of some lattice structures [3]–[5]. However, there is little published work investigating lattice structures for vibration isolation and thermal expansion control; both of which are significant for precision engineering applications. Many applications need structures that can be isolated from external vibration, for example, the tool in a CNC machine and the probe of an optical metrology system. High stiffness structures are often used, which increase the natural frequency, achieving vibration damping [6]. Taking an alternative and complementary approach, this paper discusses applications of lattice structures for vibration isolation.

FIGURE 2 shows the vibration response of a structure, with natural frequency f_n to an external vibration source with frequency f . When $f_n = f$, a resonance occurs, leading to a large displacement amplitude. [6]. To have higher vibration isolation efficiency, a structure should have a low f_n, which can be achieved by lowering the stiffness of the structure. But, there is a practical limit: if the stiffness is too low, the structure will be unable to sustain the mass load of the body of interest (work tool/probe). Lattice structures possess high strength-to-weight ratio for their mass, providing low stiffness at relatively high strength [1].

In this study, various configurations of strut-based lattice structure are investigated with a combination of finite element analysis (FEA) and experimental assessment. Information gained in this study shows that lattice structures can be used to tune the design of a structure to have a desired f_n for a specific vibration isolation application, effectively setting up a mechanical

band-gap. In practice, external vibration sources commonly have multiple dominant frequencies, so f_n should be optimised for a specific range of frequencies. A case study in which a metrology frame for an optical system is to be designed, will be used to demonstrate how f_n for the lattice structures can be optimised for a specific frequency range.

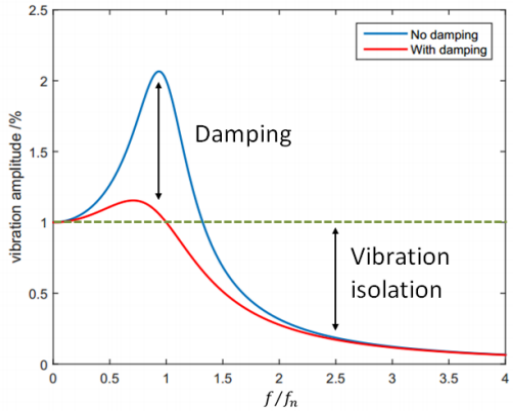

FIGURE 2. Vibration damping and isolation.

LATTICE DESIGN AND FABRICATION

Strut-based lattices are used in this study as they are periodic open-cell cellular structures that possess bending characteristics that give longer plateau regions than closed cell cellular structures, and thus can absorb more energy than periodic closed-cell cellular structures [1],[7].

CAD design

The design of lattice structures for AM poses a significant challenge. We have developed a simple design tool, in the form of equation (1). This allows us to construct a range of lattice unit cells with predefined volume fraction, *V*. Lattice strut diameters were calculated using equation (1), thus

$$d^3\left(\pi\left(\frac{a_2}{16}+\frac{a_3}{16}+\frac{b\sqrt{2}}{8}+\frac{c\sqrt{3}}{4}+e\right)\right) + d^2\left(S_l\pi\left(\frac{a_1}{16}+\frac{a_2}{16}+\frac{a_3}{16}+\frac{b\sqrt{2}}{8}+\frac{c\sqrt{3}}{4}\right)\right) - V = 0 \quad (1)$$

where the length of a unit cell is fixed at 30 mm; d is the strut diameter; S_l is the cell length; a_1 is the number of horizontal struts of length S_l as they appear in top and bottom views of a single lattice cell; a_2 is the total number of vertical struts of length C_l as they appear in top and bottom views of a single lattice cell; a_3 is the total number of vertical struts of length C_l as they appear in front, back and side views; b is the total number of diagonal struts on all faces; c is the number of diagonal members across the centre of the lattice cell; V is the filled volume of the lattice cell; and e is the constant of intersection volume equal to 0 when c = 0, 0.181021 when c = 2, and 0.636638 when c = 4 [8].

CAD was used for the design of single unit cells which were then tessellated to create lattice structures (as illustrated in *FIGURE* 3).

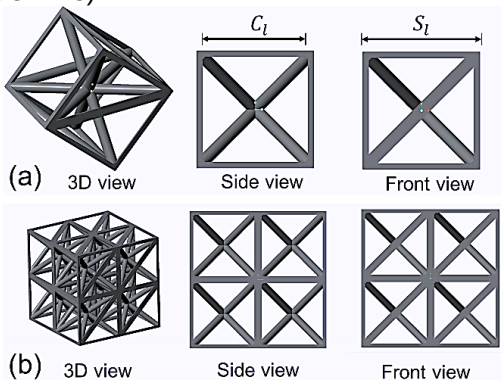

FIGURE 3. (a) Example of single lattice cell as designed with Creo Parametric CAD software, and (b) example of 2×2×2 periodic lattice cells as tessellated with Autodesk Inventor CAD software.

Samples with lattice behaviour

There is a minimum required number of lattice unit cells that a structure should have in order for it to exhibit lattice behaviour, hence, the designed lattices should be tested to determine whether they exhibit lattice behaviour [9]. Experimental compression tests were carried out on samples of similar overall size, volume fraction and, cell configuration, but of variable number of tessellations: 2×2×2, 3x3×3 and 4×4×4. The samples are shown in FIGURE 4. The purpose of these experimental compression tests is to determine the minimum number of cells that represent a lattice structure, which will later be used in the study.

Three replicas of each sample were compressed at a constant compression speed of 1 mm·min^{-1}. The results of the compression tests with the three samples are shown in the form of load-displacement curves in

FIGURE 5. All samples took the curves up to the densification area, which essentially means all tested samples exhibited lattice behaviour. This means that 2×2×2 lattices represent the minimum number of lattices that can be used in this study.

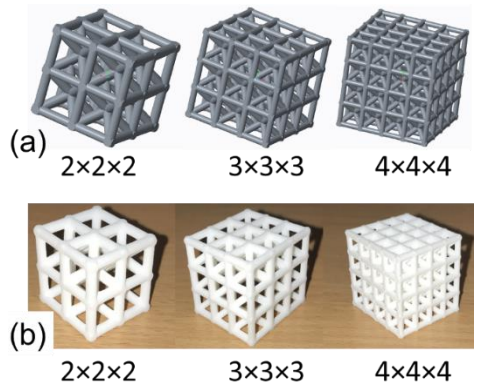

FIGURE 4. (a) Design of compression test samples, and (b) compression test samples as manufactured from Nylon 12 powder on an EOS P100 selective laser sintering machine with a building powder layer height of 100 µm.

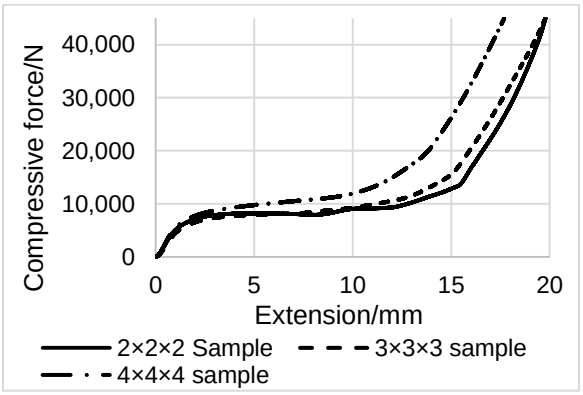

FIGURE 5. Compression test curves of lattice samples of different unit cells.

Lattice structure identification

The lattice structures used in this study are of different volume fraction, different number of nodes and different cell configurations. For the purpose of individual characterisation, every lattice cell was assigned a unique code in the form of ($x_1x_2x_3x_4$-x_5), where $x_1$is the number of nodes in a 2D view of the single cell, $x_2x_3x_4$ denotes the volume fraction taking, for example, a value of '010' for a 10 % lattice cell, and x_5 is an identification number of the struts configuration. A total of twenty-three lattice cell configurations were developed based on a fixed number of nodes. Each configuration formed the basis for three different volume fraction cells: 10 %, 20 % and 30 %. FIGURE 6 shows the lattice cells of 10 % volume fraction in a 2×2×2 tessellation.

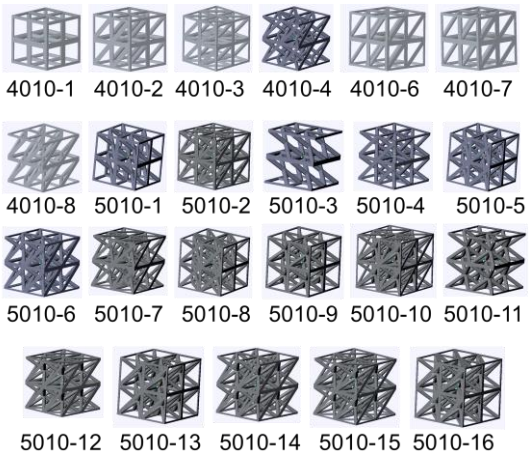

FIGURE 6. CAD models of the lattices used in this study, all in 2×2×2 tessellation and of 10 % volume fraction.

MODELLING ISOLATION PROPERTIES

The CAD models shown in FIGURE 6, along with their corresponding versions of 20 % and 30 % volume fraction, were analysed using ANSYS Workbench FEA. To ensure the calculations had converged with respect to the element size, we determined the first f_n of the structures using a range of element sizes from 25 mm to 0.25 mm. At an element size of 1 mm, the difference between subsequent results had fallen below 1 % for Nylon-12 samples of (60×60×60) mm size. Therefore, we used elements of 1 mm for all subsequent calculations. The base surfaces of the models were constrained in all degrees of freedom. The harmonic response to a vertical load of 0.1 N, vibrating at a frequency in the range 0.1 Hz to 1000 Hz (with 10 Hz frequency intervals) acting on the upper surface was simulated. The displacements due to the generated harmonic vibration in the vertical direction were calculated. The simulated spectra of the 4010-x and 5010-x lattice models are shown in FIGURE 7, where the peaks represent f_n of each model. The 5010-x lattice types have peaks at higher frequencies than the corresponding 4010-x lattices with the same number of unit cells, except for the 5010-3 lattice, which has the lowest natural frequencies among all the tested samples. This makes the 5010-3 cell a good candidate for vibration isolation. However, the 5010-3 cell has more resonance frequencies within the testing range than the

4010-8 cell. Consequently, the 5010-3 cell can complicate the control of vibration isolation because the 5010-3 cell has high number of resonance peaks that need to be controlled for providing vibration isolation, and thus, the 4010-8 cell is more appropriate for vibration isolation control.

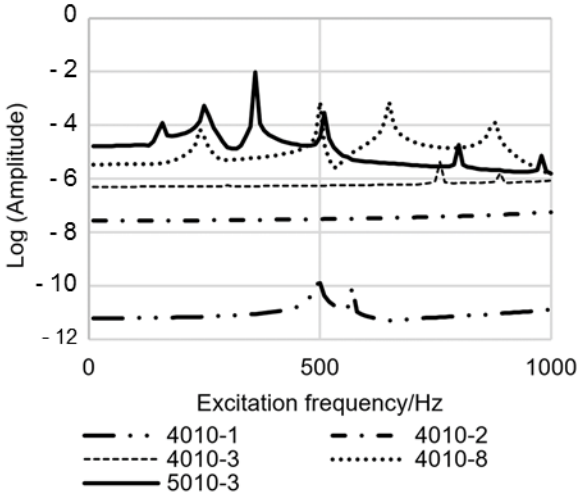

FIGURE 7. Results from harmonic response simulations of the 4010-x and 5010-x lattice types in 2×2×2 tessellations.

The models with lower volume fraction showed lower natural frequencies than models of higher volume fraction. This is most likely due to the lower stiffness of the lower volume fraction models.

For experimental verification of these results, three samples each of the 4010-8 and 4030-1 lattices were manufactured and the harmonic responses in the vertical direction were tested. Each sample was fixed to a shaker (shown in FIGURE 8) which vibrated in the range of 0.1 Hz to 1000 Hz for the 4010-8 samples, and a range of 0.1 Hz to 3000 Hz for the 4030-1 samples (all with < 1 Hz frequency intervals) and the reaction of the bottom surface of the sample was measured using a force sensor attached to the shaker. The frequency range for the experimental testing of each sample was chosen based on the range at which f_n was obtained using FEA for each sample. The positions of the natural frequency peaks are in 90.6 % average agreement with the frequencies at which they appeared in the simulation results. Comparison between average experimental results and simulation results are shown in FIGURE 9.

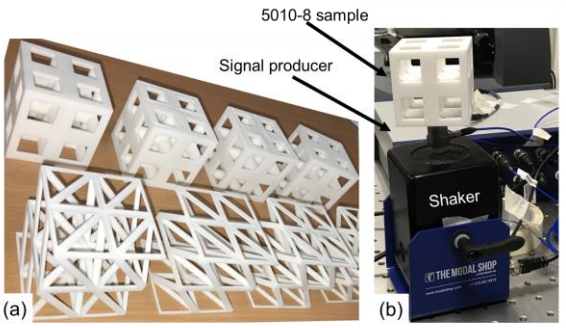

FIGURE 8. (a) Selective laser sintering manufactured samples for experimental verification, (b) vibration experiment setup.

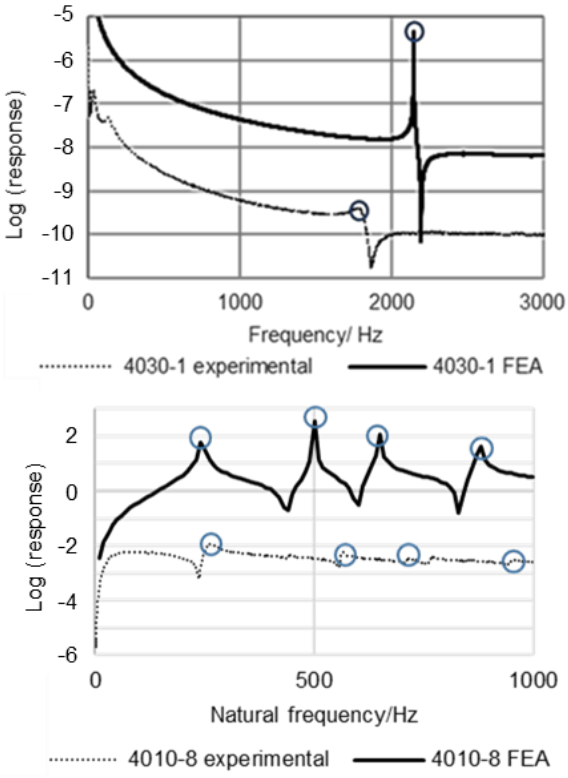

FIGURE 9. Experimental verification of the natural frequencies for vertical excitation of the 4030-1 (top) and 4010-8 (bottom) lattice structures.

The effect of the size of the lattice cells on the natural frequencies was simulated. The following sizes were chosen: 30 mm, 22.5 mm and 16.875 mm, while keeping the number of tessellations constant at 2×2×2. From the FEA results, it can be concluded that decreasing the cell size results in higher natural frequencies. This is likely due to the excitation of shorter wavelength vibration modes than are permitted in

larger structures of the same volume fraction, as shown in FIGURE 10.

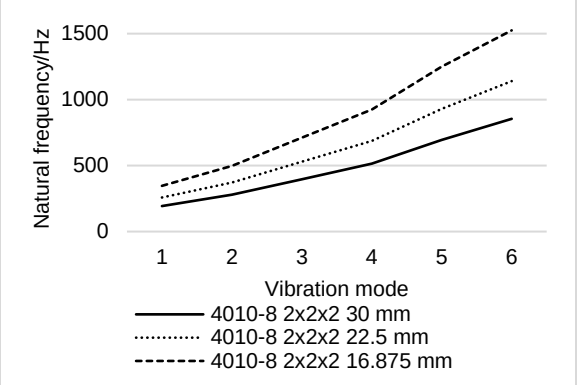

FIGURE 10. The effect of lattice cell size on f_n.

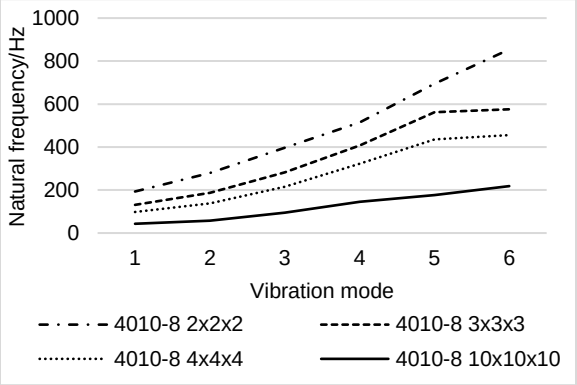

FIGURE 11. The effect of the number of tessellations of lattice cells on f_n.

In addition, increasing the number of tessellations, for a constant cell size and volume fraction, reduces f_n of the structure, which is thought to be related to increased strut bending in structures with a higher number of tessellations. This was confirmed by testing samples of tessellations of 2, 4, 5 and 10, in three-dimensions, as shown in FIGURE 11.

CASE STUDY

The structural frame of a new all-optical coordinate measuring system was manufactured with selective laser sintering from Nylon-12 using lattice structures to hold the mass of a 1 kg probe and isolate mechanical vibrations in the z-direction arising from the movement of the stage which drives the probe, which vibrates in the range from 40 Hz to 80 Hz.

Determining the lattice cell size

There are two options for the selection of the cell size and number of cell tessellations that can fill a volume in space with low f_n: (a) large size cells with low number of tessellations, or (b) smaller cells with a higher number of tessellations. The results, so far, do not suggest which route is more appropriate. As a result, a study was conducted with the aim of suggesting the most appropriate route to obtain lower f_n. The study comprised the design of (30×30×30) mm lattice structure samples using 4010-8 cells of different sizes: 15 mm, 7.5 mm, and 3.75 mm. By default, cells of less size need a higher number of tessellations to fill the (30×30×30) mm space. FEA (results are summarised in TABLE *1*) showed that larger size cells had lower first mode f_n than smaller ones with a higher number of tessellations.

TABLE 1.The coupled effect of cell size and number of tessellations at constant volume fraction on the first f_n of the lattice structures.

Cell size/ mm	Sample size/mm	Number of cells	1st mode f_n/ Hz
15	30	8	409.97
7.5	30	64	421.51
3.75	30	512	467.88

As a result, the most suitable cell size for the structural frame must have two tessellations in the direction of the shortest dimension (two is the lowest number of tessellations that can represent a lattice as discussed previously). Subsequently, 30 mm cells were used to construct the body of the structural frame because the shortest dimension was the thickness of the structural frame (60 mm). The structure used the 4010-8 cell, for the reasons discussed above, and then varied the volume fraction, and the number of tessellations to get the isolation to the desired range.

Verification with in-situ harmonic test

The design of the structural frame comprises three identical sub-frames each kinematically coupled to the stage of the optics through balls in v-grooves located on top of each sub-frame. The sub-frame, shown in
FIGURE 12, is stiffened at the back through the use of a solid swept stiffener, and in both sides through the use of perforated swept surfaces to further damp the vibration in x- and y- directions. The harmonic response to the compressive working load of 10 N, with excitations ranging from 0.1 Hz to 1500 Hz, was modelled with frequency intervals of 1 Hz. A safety factor of two was used for the maximum working load which was applied to the top of the frame.

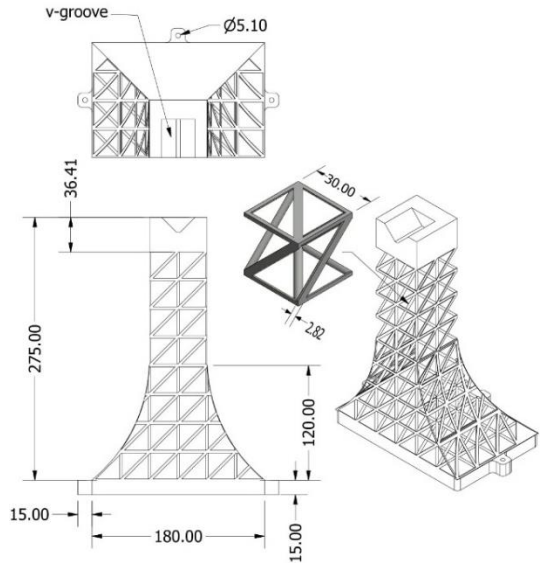

FIGURE 12: Design of the structural sub-frame for isolating vertical excitations arising from the movement of the stage of the optics using lattice structure, dimensions in millimetres.

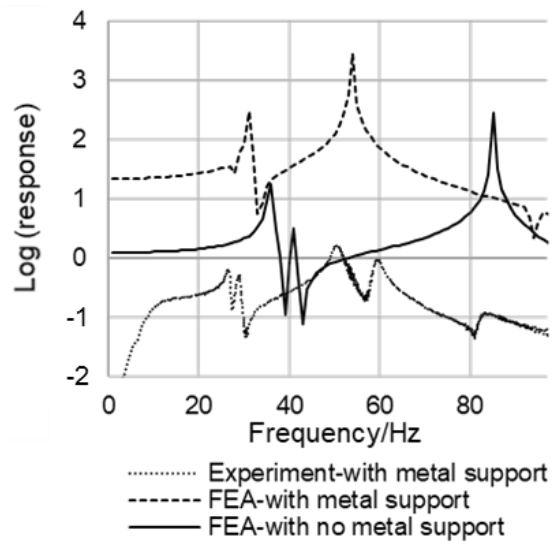

FIGURE 13: Harmonic response of one sub-frame.

The structure succeeds in isolating excitations in the range of 38 Hz and 83 Hz, with maximum displacement of 2 % of the length of the frame, see
FIGURE 13. Additional metal support was used to mount the sub-frame on the shaker which affected the harmonic results obtained from experiment. The positions of f_n peaks from FEA of similar conditions to the conditions of the experiment are in 89.8 % average agreement with the frequencies at which they appeared in the experiment results.

CONCLUSION

Before lattice structures can be used for vibration isolation of a system, the dynamic behaviour of the system has to be understood. Then, the lattice characteristics can be tailored to isolate the resonance peaks of the system. The control of the natural frequency is the major step towards tailoring the lattice structure. The study reveals that the natural frequency of a lattice structure can be reduced by increasing cell size, reducing volume fraction, and/or increasing the number of tessellations of a singular lattice cell, and vise versa. The work was funded by the EPRSC project EP/M008983/1.

REFERENCES

[1] L. J. Gibson and M. F. Ashby. Cellular Solids: Structure and Properties. Cambridge University Press, Cambridge: 1999.

[2] O. Rehme and C. Emmelmann. Rapid Manufacturing of Lattice Structures with Selective Laser Melting, Proc. SPIE 2006; 6107:192-203.

[3] C. Yan, L. Hao, A. Hussein, P. Young, and D. Raymont. Advanced Lightweight 316L Stainless Steel Cellular Lattice Structures Fabricated via Selective Laser Melting, Mater. Des. 2014; 55: 533-541.

[4] C. Yan, L. Hao, A. Hussein, and D. Raymont. Evaluations of Cellular Lattice Structures Manufactured Using Selective Laser Melting, Int. J. Mach. Tools Manuf. 2012; 62: 32-38.

[5] M. Santorinaios, W. Brooks, C. J. Sutcliffe, and R. A. W. Mines. Crush Behaviour of Open Cellular Lattice Structures Manufactured Using Selective Laser Melting, WIT Trans. Built Environ. 2006; 85: 481-490.

[6] T. L. Schmitz and K. S. Smith. Mechanical Vibrations: Modeling and Measurement. Springer, New York: 2011.

[7] O. Rehme. Cellular Design for Laser Freeform Fabrication. Gottingen: 2010.

[8] M. Moore. Symmetrical Intersections of Right Circular Cylinders, Math. Gaz. 1974; 58: 181-185.

[9] W. P. Syam, J. Wu, B. Zhao, I. Maskery, W. Elmadih, and R. K. Leach. Design and Analysis of Strut-based Lattice Structures for Vibration Isolation. Precision Engineering. 2017; In press.